STATISTICAL AND METALLOGRAPHIC VIEWS ON QUANTIFICATION OF INTERMETALLIC PHASES IN AUSTENITIC STAINLESS STEELS

Lucie Pilsová, Anna Altová, Vladimír Mára

Abstract

This article deals with the metallographic evaluation of SUPER 304H austenitic stainless steel, which is mainly used in energetics. The experimental material is in the state after long-term laboratory aging, which simulates the effect of increased temperature during real operation in a power plant. New phases are formed in the material, the amount of which can be determined by evaluating their area fraction on the optical micrographs. In the first place, the results can be influenced by the choice of etching method during metallographic preparation. The results of the following thresholding are often interpreted without verifying the validity of the data using statistical methods. Therefore, we introduce simple statistical analysis to check for the normal distribution of the data. The results of this analysis imply that there is either a combination of two morphological types of the present phase, or its incorrect differentiation from the carbidic particles.

Keywords: *metallography, thresholding, image analysis, austenitic stainless steel, sigma phase, Shapiro-Wilk test*

1 INTRODUCTION

SUPER 304H steel is used in the energy industry for steam reheaters and superheaters. It is intended for the so-called supercritical cycles of coal-fired power plants, which work with higher efficiency than conventional power plants. The material must withstand a temperature above 650 °C at a medium pressure of approx. 25 MPa. In the as-received state, the material consists of an austenitic matrix with strengthening primary carbonitrides Nb(C,N) and uniformly distributed Cu nanoparticles, which improve creep properties. When exposed to temperatures in the range of 550-600 °C, chromium carbides, mostly $M_{23}C_6$ type, are formed especially along the grain boundaries, which cause the materials embrittlement. With a temperature of 600 °C (according to some sources 650 °C), the growth of the sigma phase is activated. It is an intermetallic, in the case of SUPER 304H steel, composed of Cr, Fe, Ni and, possibly, other trace elements. The sigma phase forms at the triple junction of grain boundaries, in areas rich in Cr. However, it can also occur in the matrix, where its encrustation around the primary Nb(Cr, N) phase is a frequently observed phenomenon. Indirectly, the presence of the sigma phase can be observed by an increase in hardness, strength and a decrease in yield strength and ductility. (Masuyama, 2001; Huang et al., 2018; Kuboň, 2014)

The issue of sigma phase growth as a result of temperature exposure was widely discussed, for example, in Korea (Le et al., 2020), China (Ni et al., 2016) and Poland (Zieliński et al., 2022). Since 2011, follow-up research (Sawada et al., 1986) on the creep resistance of S304H steel has been continuing as part of the NRI Datasheet project in Tsukuba, Japan. Since 1997 this steel has been used as a material for superheater pipe systems in most Japanese coal-fired power plants (Sakai et al., 1998). However, no statistical method was used for determining the area fraction of particles in the articles mentioned above, at most with the exception of stating the standard deviation.

To determine the amount of sigma phase, image analysis is used on micrographs from an optical light (LOM) and scanning electron microscope (SEM). An example of particle thresholding (image segmentation) from the electron microscope micrograph is shown in Fig. 1.

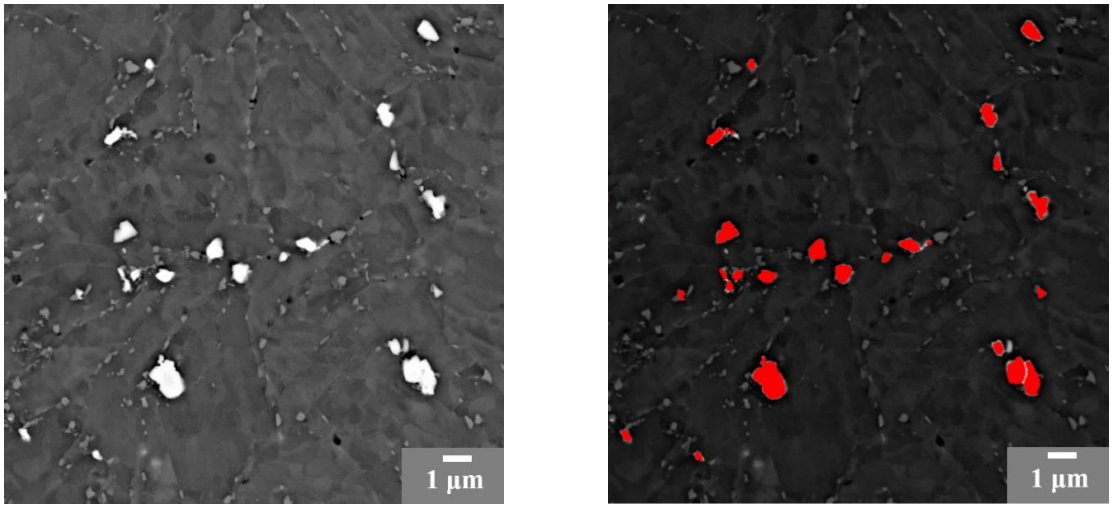

Fig. 1: Particle thresholding in the SEM image

In technical practice, thresholding methods from light microscopy images are often used, but less often the statistical significance of the selected number of images and the appropriate optical magnification is verified. Since the chemical composition of the particles cannot be known from the light microscope by its definition, it is difficult to distinguish them during the thresholding. This article does not provide a one-size-fits-all solution, rather it combines standard metallography and image processing with basic statistical methods that should be included in the daily image analysis routine in the laboratory.

It is not only for LOM that it is important to choose a suitable type of microstructure highlighting - etching. Electrolytic etching in a 10% aqueous oxalic acid solution is often used for austenitic steels. This method usually highlights grain boundaries, but it penetrates deeper and can lead to a to extraction of particles from the matrix. This can subsequently be a problem for electron microscopy and EDXS (Energy Dispersive X-ray Spectrometry) analysis. However, electrolytic etching can also take place in sodium hydroxide solution, where phases rich in Cr are appropriately highlighted after etching.

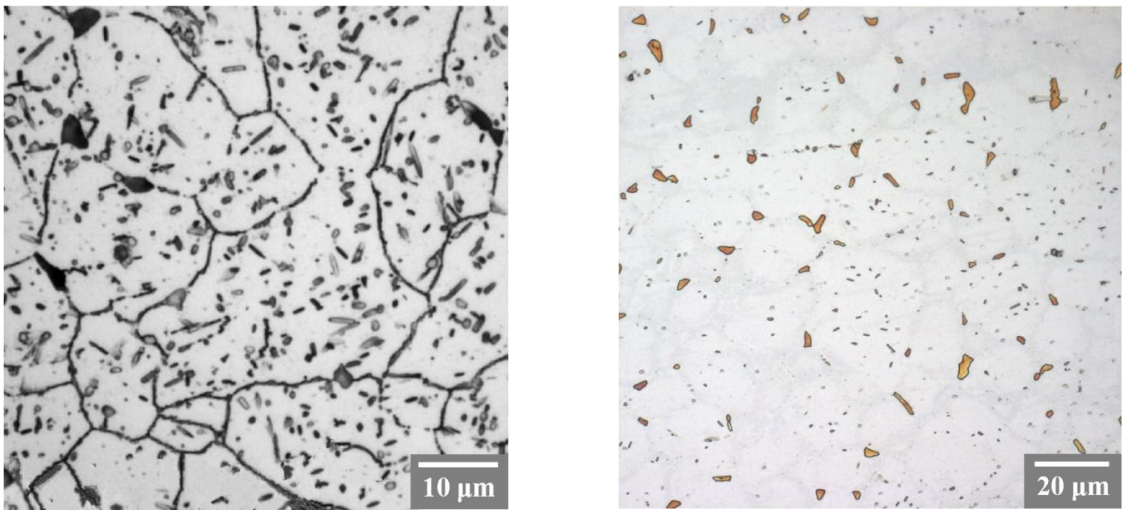

Fig. 2: LOM micrograph of electrolytically etched microstructure with (a) 10% aqueous solution of oxalic acid and (b) with 20% aqueous solution of NaOH

2 METHODS AND MATERIALS

2.1 Experimental material

Super 304H steel belongs to the group of so called "younger materials" (first data from 1986 (Abe and Kern, 2008)) type 18Cr-9Ni which is used in coal-fired power plants mainly as a part of the heat exchange surfaces of heaters and steam reheaters.
The chemical composition of the supplied reheater tubes is given in Tab. 1.

Tab. 1: Chemical composition of SUPER 304H steel samples (wt. %)

C	Si	Mn	P	S	Ni	Cr	Nb	Cu	N	B	Al
0.08	0.21	0.082	0.033	-	8.9	18.4	4.9	3.00	0.11	0.004	0.008

Specimens in the form of tubes were long-term laboratory exposed to elevated temperatures of 650, 675 and 700 in electric resistance furnaces in air. The metallographic samples were fixed in phenolic resin, ground on standard SiC papers, polished using a colloidal solution of 0.05 μm Al_2O_3 and etched with a 10% oxalic acid water solution at 10 V for 5-10 s.

2.2 Experimental data

The data sets contain data obtained by image analysis of microstructure images taken by the Neophot32 light optical microscope equipped with CCD camera. The thresholding image analysis was performed in the NIS Elements (version 3.5 AR) program.
The following Tab. 2 provides an overview of all available datasets for each exposure, as well as highlighting in grey those that were used for the purposes of this article.

Tab. 2: Datasets obtained from the image analysis

Set no.	1	2	3	4	5	6	7	8
Exposure temperature (°C)	650	650	675	675	675	675	700	700
Exposure time (10^3 h)	15	24.5	12	15	20	24.5	15	24.5

From the image analysis, the parameters Area (μm^2), Width (μm), Length (μm), Temperature (°C) and Time (10^3 hours) were used for the purposes of this work. Each set of data is further divided into two groups, according to the heat treatment. The author of (Horváth, 2018) hypothesized that prior annealing could make the material susceptible/resistant to sigma phase growth. In the same work (Horváth, 2018), it is stated in the conclusions that the effect of heat treatment is negligible, and therefore the specimens state (Z – normalizing annealing, N – not annealed) was not taken into the account here. R (version 4.2.1, Funny-Looking Kid) analytical software was used for statistical calculations and plotting the graphs.

2.3 Physical-material background for later hypotheses

It is necessary to point out some of the generally valid principles that govern the growth of this type of phases in general. Thermodynamic changes always take place in the least energy-demanding conditions, i.e. situations where their activation enthalpy reaches the lowest values compared to other, theoretically permissible events. This also applies to the growth of the sigma phase - the beginnings of its formation start where the grain boundaries are weakened in some way (for example, by the previous presence of Cr carbides) and where is also more Cr present than in the surrounding matrix. (Hsieh and Wu, 2012; Cahn and Haasen, 1996).

The sigma phase most often grows in directions perpendicular to the applied load, if it is present (it was not in the analyzed samples). Then it grows in the direction of least resistance, i.e. from the point of triple contact of grains further along the grain boundaries and possibly connecting with other sigma phase nuclei and thus forming needle-like formations which can be observed in cross-section. (Zhou et al., 2019) This fact is important for the later established hypotheses – the sigma phase thus extends its longitudinal dimension, and the length to width ratio also increases. The area of the sigma phase also increases, but these values cannot be interpreted without the context of the phase dimension, as other phases present in other materials may grow more spheroidally and the ratio of width and length for the same area can be close to 1.

3 RESULTS

3.1 Graphical analysis of input data

A useful basis for the formulation of hypotheses is the graphical representation of the data in histograms, as shown in Figs. 3 - 7.

It can be seen from Fig. 3 that the largest representation has particles with a surface area of approximately 2 μm^2.

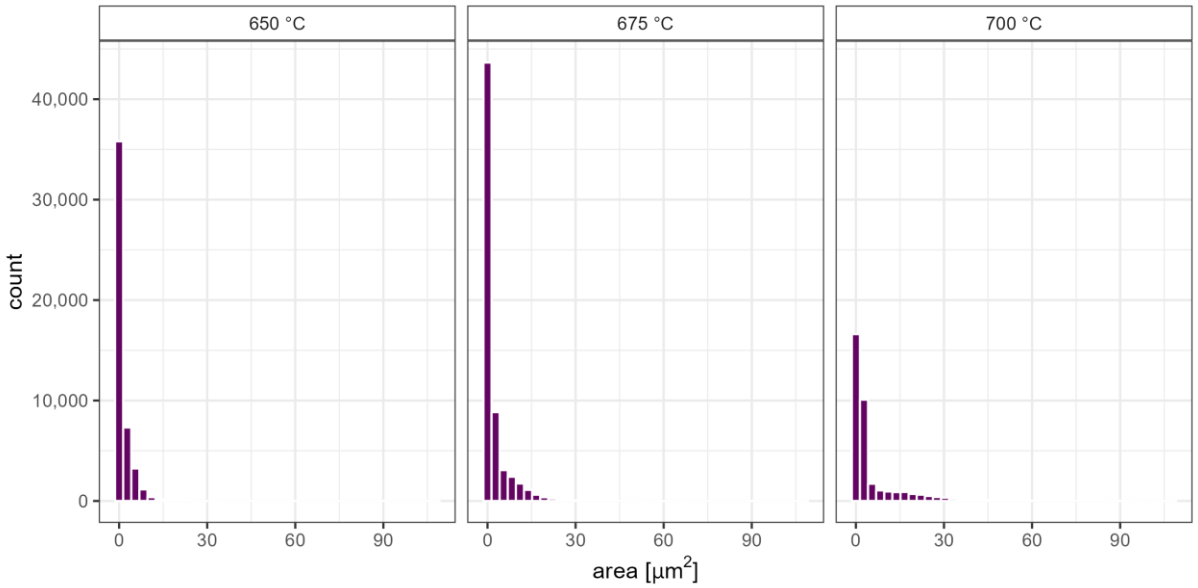

Fig. 3: the total number of particles represented by their area

When taking the logarithm of the Area on the x-axis, the right skewed bimodal character of the distribution can be observed. This may indicate that more than one phenomenon may have been captured by thresholding the image (in practice, this may be more particle types).

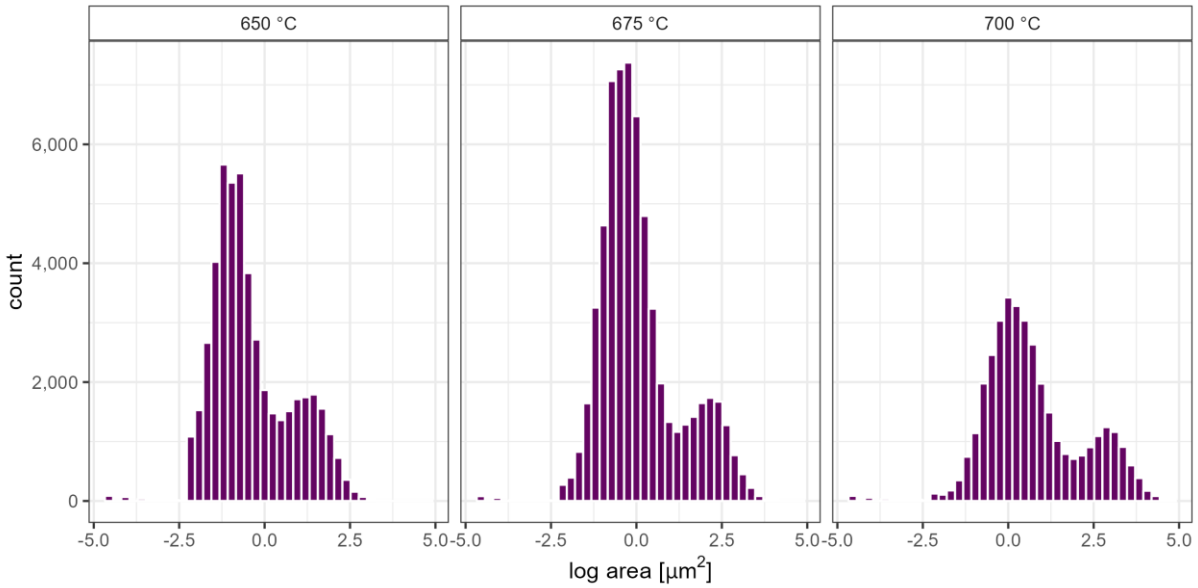

Fig. 4: the total number of particles represented by their area with the logarithm of the x-axis values

The graph in Fig. 5 was constructed from a selection of data that are longer than 10 µm for all three groups covering temperatures of 650, 675 and 700 °C. Based on the observations, progressively larger particles of the increasing sigma phase should appear in the microstructure with increasing temperature. Therefore, the representation of particles larger than 10 micrometers, which are clearly identifiable on a light microscope, was plotted. However, this filtering does not include distinguished particles based on their chemical composition. This is only possible in images taken with an electron microscope.

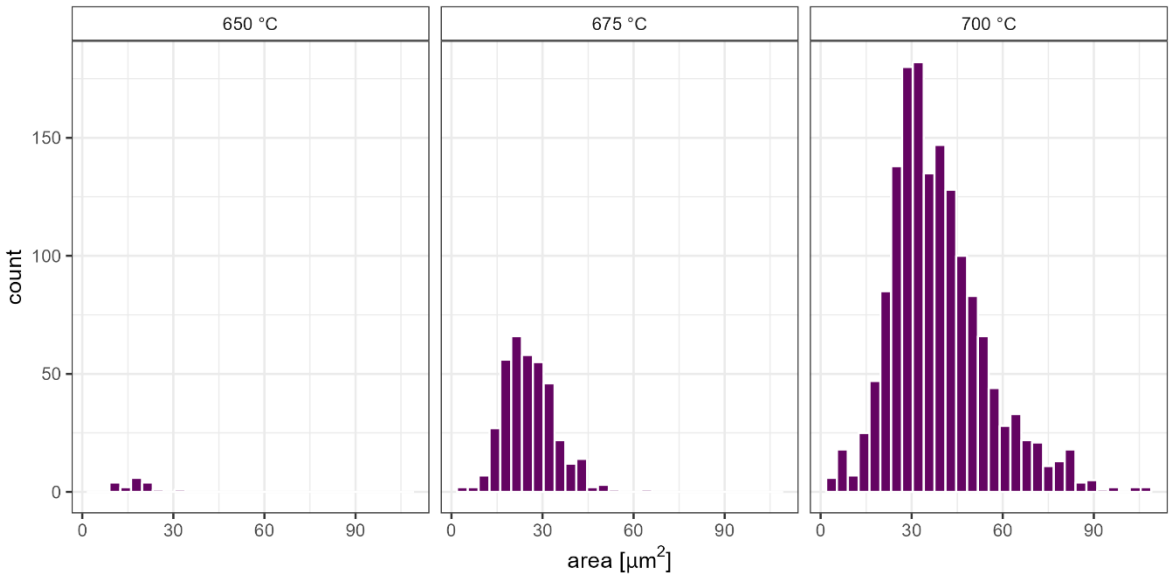

Fig. 5: Number of particles > 10 µm in length

From the graph in Fig. 5, it can be concluded that in the examined samples, with increasing temperature, far more particles with a larger area than at the beginning began to appear. At the same time, by filtering according to the length greater than 10 µm, it is guaranteed that rather elongating particles are displayed in the graph. However, in order to make the trend even easier to follow, a graph was drawn (Fig. 6) which shows the representation of all lengths

(here represented by the width/length ratio – i.e. the larger the ratio, the more evident that the sigma phase is lengthening in one direction) in individual exposure temperatures.

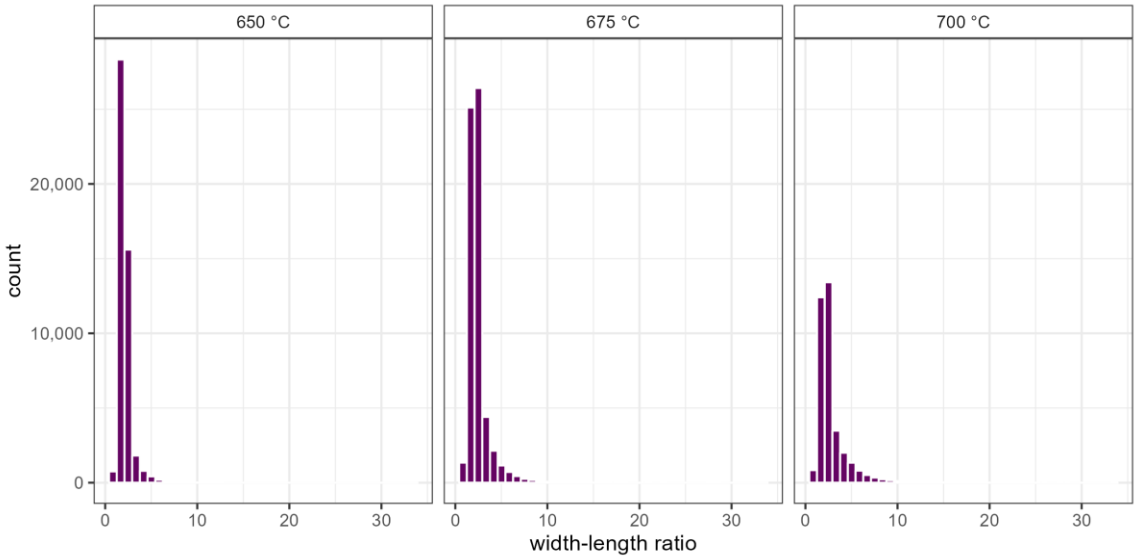

Fig. 6: Histogram of the all particles according to the ratio of their width and length

The graph in Fig. 6 shows that the largest number of particles have a ratio of w/h less than 10. Therefore, for a more detailed investigation, another graph (Fig. 7) was drawn with the criterion to display only those particles whose ratio w/h < 10.

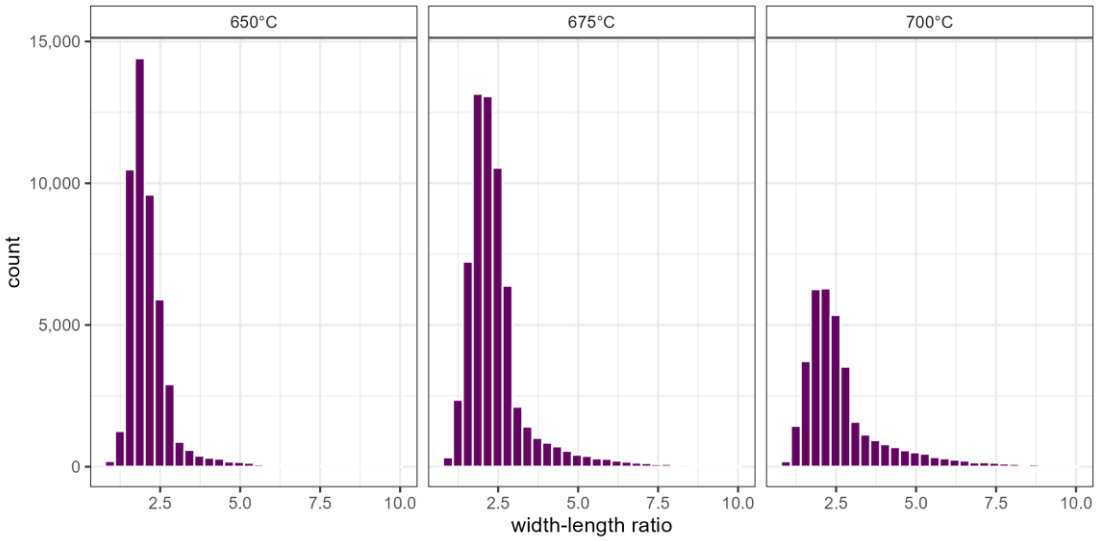

Fig. 7: Histogram of the particles according to the ratio of their width and length lesser than 10

3.2 Statistical analysis

From the selected data series, only those items whose dimension corresponded to the formula Length > 10 μm were selected for further calculations.

Using the ANOVA (analysis of variance) method, we wanted to find out whether the variability of the phase Area (μm^2) corresponds only to random fluctuations, or whether it also shows a different level of values in different groups sorted according to the analysed factor – here temperatures (°C).

3.3 Verification of the conditions for the use of ANOVA

In general, to perform any statistical analyses, the data should be a representative sample, which means that, based on common parameters, such a number and species must be selected that generally valid conclusions can be interpreted based on the results (Dohnal, 2020). More easily determined metrics for verifying the use of the ANOVA method are in particular: data normality and homoscedasticity.

Data normality

A basic overview of the normal distribution of data is a histogram showing probability density distribution of the measured data. It was found that the original measured data did not show a normal distribution (Fig. 8).

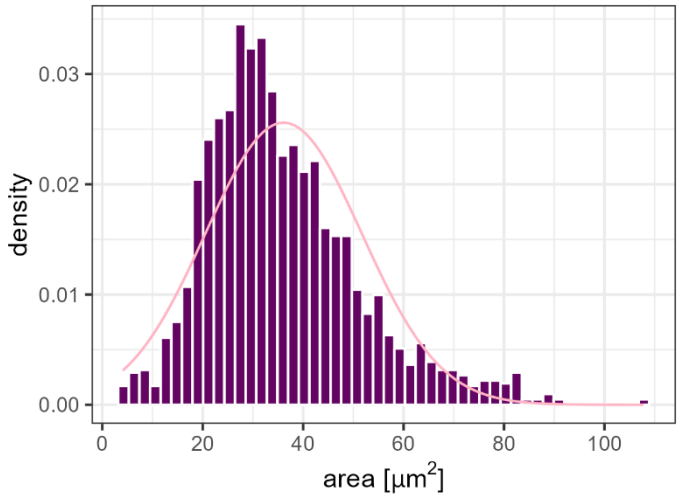

Fig. 8: The data normality evaluation

Another indicator of normality can be, for example, the Shapiro-Wilk test as seen in Fig. 5. The test's results showed non-normal distribution of the data ($W = 0.95$, p-value < 0.001). The test was performed on data sets with lengths > 10 μm.

The solution may be to transform the data, for example by natural logarithm. The ANOVA method could therefore be used on transformed data, but it is also necessary to test their homoscedasticity. This is a property of data where variances between individual groups are identical (similar). Since the ANOVA method works precisely with variances, their differences would lead to a distortion of the result of the entire analysis (Dohnal, 2020).

For checking for homoscedasticity, we employed the Levene's test, which tests the equality of variances of two or more (in our case three) groups. The results of the test ($F = 48.98$, $p \leq 0.001$) imply the rejection of the null hypothesis, which means the condition of homoscedasticity is not fulfilled.

4 DISCUSSION

From the graphical comparison of the three exposure temperatures, the distribution of the particle size was evident. The highest number of particles had an area around 2.5 μm^2 (Fig. 3). It was also possible to estimate from the histograms that the number of large particles increases with temperature and that they probably growing in length in one direction (Fig. 5). However, this could not be unequivocally confirmed when drawing histograms (Figs. 6 and 7), where the criterion was circularity (ratio w/h) of the particles.

5 CONCLUSIONS

Images taken with a light microscope indicated that increasing exposure temperature probably has an effect on the growth of the sigma phase. Samples after temperature exposure for 24,500 h at 650, 675 °C and 700 °C were selected for image analysis.

Using the Shapiro-Wilk test, it was determined that the analyzed data did not completely follow a normal distribution. Therefore, the Area data was corrected by the natural logarithm. Although the data then showed a normal distribution, it did not meet the second condition, namely the equality of variances between groups (homoscedasticity).

For further research, it will be necessary to try, for example, a larger number of images, but at a higher optical magnification. Try a different etching method and especially combine it with verification by determining the chemical composition on an electron microscope with the appropriate detectors.

The main conclusion of this article is, in particular, the finding that it is necessary to subject even basic results from commonly used methods to critical examination.

Acknowledgements

The measured data were provided by Ing. Jakub Horváth, Ph.D.

References

1. ABE, F. and KERN, T. (eds.), 2008. *Creep-resistant steels*. . Boca Raton, Fla.: CRC Press. Woodhead publishing in materials. ISBN 978-1-84569-178-3.
2. CAHN, R.W. and HAASEN, P.(eds.), 1996. *Physical metallurgy Volume 3*. 4th, rev.enhanced ed. Amsterdam ; New York: North-Holland. ISBN 978-0-444-89875-3.
3. DOHNAL, G., 2020. XII. Testování hypotéz. Online. Praha. 21 September 2022. Available from: https://sms.nipax.cz/_media/ps_20_11_testy_hypotez.pdf
4. HORVÁTH, J., 2018. *The structural stability of creep resistant austenitic steels SUPER 304H and Tp 347HFG*. Online. Disertační práce. Praha: ČVUT. [Accessed 26 October 2022]. Available from: https://dspace.cvut.cz/handle/10467/78610
5. HSIEH, C. and WU, W., 2012. Overview of Intermetallic Sigma Phase Precipitation in Stainless Steels. *ISRN Metallurgy*. 2012. Vol. 2012, p. e732471. DOI https://doi.org/10.5402/2012/732471.
6. HUANG, X., ZHOU, Q. and WANG, W., 2018. Microstructure and property evolutions of a novel Super304H steel during high temperature creeping. *Materials at High Temperatures*. 3 September 2018. Vol. 35, no. 5, p. 438–450. DOI 10.1080/09603409.2017.1376831.
7. KUBOŇ, Z., 2014. New Austenitic Creep Resistant Steels for Superheaters of USC Boilers. *Key Engineering Materials*. December 2014. Vol. 635, p. 75–80. DOI 10.4028/www.scientific.net/KEM.635.75.
8. LE, T.G., YOON, K. B. and MA, Y. W., 2020. Metal Temperature Estimation and Microstructure Evaluation of Long-Term Service-Exposed Super304H Steel Boiler Tubes. *Metals and Materials International*. Online. 15 July 2020. [Accessed 16 September 2022]. DOI 10.1007/s12540-020-00808-4.
9. MASUYAMA, F., 2001. Advances in Physical Metallurgy and Processing of Steels. History of Power Plants and Progress in Heat Resistant Steels. *ISIJ International*. 2001. Vol. 41, no. 6, p. 612–625. DOI 10.2355/isijinternational.41.612.
10. NI, J., LI, H., LI, M. and WANG, Z., 2016. Research on Microstructure Transformation of Super304H Stainless Steel in the Process of Aging at 700. In: *International Conference on Education, Management, Computer and Society*.

Online. Atlantis Press. January 2016. p. 1974–1978. [Accessed 15 September 2022]. ISBN 978-94-6252-158-2. DOI 10.2991/emcs-16.2016.496.
11. SAKAI, K., MORITA, S., YAMAMOTO, T. and TSUMURA, T., 1998. Design and Operating Experience of the Latest 1,000-MW Coal-Fired Boiler. *Hitachi Review*. 1998. Vol. 47, no. 5, p. 5.
12. SAWADA, K., KIMURA, K., ABE, F., TANIUCHI, Y., SEKIDO, K., NOJIMA, T., OHBA, T. and WATANABE, T., 1986. *Data Sheets on the Elevated-Temperature Properties of 18cr-8ni Stainless Steel for Boiler and Heat Exchanger Seamless Tubes (SUS 304HTB)*. National Institute for Materials Science.
13. ZHOU, Q., LIU, J. and GAO, Y., 2019. An insight into oversaturated deformation-induced sigma precipitation in Super304H austenitic stainless steel. *Materials & Design*. 5 November 2019. Vol. 181, p. 108056. DOI 10.1016/j.matdes.2019.108056.
14. ZIELIŃSKI, A., WERSTA, R. and SROKA, M., 2022. The study of the evolution of the microstructure and creep properties of Super 304H austenitic stainless steel after aging for up to 50,000 h. *Archives of Civil and Mechanical Engineering*. 14 March 2022. Vol. 22, no. 2, p. 89. DOI 10.1007/s43452-022-00408-6.

Contact

Ing. Lucie Pilsová
CTU in Prague, Faculty of Mechanical Engineering
Department of Materials Engineering
Karlovo náměstí 13, Prague 2, 120 00
Czech Republic
email: lucie.pilsova@fs.cvut.cz

Mgr. Anna Altová
Unicorn College
V Kapslovně 2767/2, Prague, 130 00
Czech Republic
email: anca.altova@gmail.com

Ing. Vladimír Mára, Ph.D.
CTU in Prague, Faculty of Mechanical Engineering
Department of Materials Engineering
Karlovo náměstí 13, Prague 2, 120 00
Czech Republic
email: vladimir.mara@fs.cvut,cz